Acta Mech 202, 1–16 (2009)
DOI 10.1007/s00707-008-0005-y

V. A. Lubarda · A. Marzani

Viscoelastic response of thin membranes with application to red blood cells

Received: 3 December 2007 / Revised: 14 January 2008 / Published online: 27 May 2008

Abstract The rate-type constitutive analysis of viscoelastic response of thin membranes, which includes an instantaneous elastic response and viscous behavior in both shear and dilatation, is developed with the aim to study the mechanical response of red blood cells. A convenient set of generalized stress and strain variables is introduced, which facilitates the derivation and integration of the governing differential equations. Gradual or sudden loading and stepwise unloading histories are considered. The performed parametric study of the mechanical response illustrates the effects of the introduced material parameters on the coefficient of viscoelastic lateral contraction and the overall membrane deformation. A closed form solution to the problem of radial stretching of a viscoelastic hollow circular membrane is derived without referral to the correspondence principle, which is of interest for the micropipette aspiration experiment of the red blood cell. The effects of the material parameters on the instantaneous elastic response and the subsequent rate of creep are discussed.

1 Introduction

The objective of this paper is the formulation of a simple rate-type constitutive analysis of viscoelastic response of thin membranes, with the application to red blood cell (erythrocyte) membranes. A study of the viscoelastic response of the erythrocyte membrane is of interest because the blood flow in capillaries is influenced by the deformability of the red blood cell, which depends on the geometry, elasticity and viscosity of its membrane. From the microstructural point of view, the cell membrane is a composite structure consisting of an outer phospholipid bilayer, transmembrane proteins, and a spectrin network attached to the cell on the inner cytoplasmic side [1]. The bulk (areal) modulus of the cell membrane is controlled mostly by the phospholipidic bilayer, while the shear modulus is determined by the elastic properties of the cytoskeleton, a two-dimensional network of spectrin strands bound to the bilayer. The viscous properties of the cell are due to glycoproteins embedded in or attached to a lipid bilayer [2]. A great amount of research has been devoted to various problems in the mechanics of the red blood cell, as evidenced by the references [3–7]. In the cell mechanics the red blood cell is visualized as a thin elastic membrane which surrounds a viscous fluid. A cell membrane is treated as a continuum in two-dimensions, with a molecular character in the third. It is assumed that the membrane cannot change its thickness in response to applied inplane stress, but can only change its inplane size and shape. In this two-dimensional continuum framework, within the surface of the cell membrane, the stresses and elastic

V. A. Lubarda (✉)
Department of Mechanical and Aerospace Engineering, University of California, San Diego, La Jolla, CA 92093-0411, USA
E-mail: vlubarda@ucsd.edu
Tel.: +1-858-5343169
Fax: +1-858-5345698

A. Marzani
Department of Structural Engineering, University of Bologna, 40126 Bologna, Italy

moduli are defined as the forces per unit length, and thus have the dimension on N/m [8]. The upper bound on the inplane Poisson's ratio is equal to 1, rather than $1/2$ as in the three-dimensional isotropic continuum elasticity.

The mechanical behavior of a thin membrane is described in the present paper by a viscoelastic model with respect to both the deviatoric and isotropic biaxial states of stress. Bending stiffness is neglected and the membrane material is assumed to be isotropic in its plane. An instantaneous elastic response to a suddenly applied stress is included in the analysis by using an elastic element that is connected in series with the Kelvin–Voigt viscoelastic element. A set of generalized stress and strain variables, defined by a weighted sum and difference of the inplane normal stresses and dilatations, is introduced, which facilitates the derivation and integration of the governing differential equations. The performed parametric study of the viscoelastic response illustrates the effects of the introduced material parameters on the coefficient of viscoelastic lateral contraction and the overall membrane deformation. It is shown that the inclusion of the instantaneous shear elasticity in the considered viscoelastic model eliminates the physically unrealistic negative values of the coefficient of lateral contraction. Motivated by the mechanical aspects of the micropipette aspiration test of a red blood cell, the complete solution for the viscoelastic response of a hollow circular membrane under uniform tension applied on its inner boundary is derived without referral to the correspondence principle, commonly used for such viscoelastic problems [9–11]. The time evolution of the radial displacement in the membrane is calculated for the selected representative values of the introduced shear parameter. The effects of the shear parameter on the instantaneous elastic response and the subsequent rate of creep are discussed.

2 Viscoelastic response of thin membranes

A cell membrane is considered whose thickness is so small that the model of continuum mechanics applies only within the plane of the membrane. Because of its negligible thickness,[1] applied forces are considered to be distributed per unit length, so that the membrane stresses σ_{ij} $(i, j = 1, 2)$ are defined by the force/length ratios, having the dimension N/m. The deviatoric parts of the stress and infinitesimal strain are accordingly

$$S_{ij} = \sigma_{ij} - \frac{1}{2}\,\sigma_{kk}\delta_{ij}\,, \quad e_{ij} = \varepsilon_{ij} - \frac{1}{2}\,\varepsilon_{kk}\delta_{ij}\,, \tag{1}$$

where δ_{ij} is the Kronecker delta ($\delta_{kk} = 2$, with the summation convention over the repeated index). Geometrically, $\varepsilon_{kk} = \varepsilon_{11} + \varepsilon_{22}$ represents the relative change of the membrane area element $\mathrm{d}A$, i.e., $\varepsilon_{kk} = \Delta(\mathrm{d}A)/\mathrm{d}A$. Since an infinitesimally thin membrane has no buckling resistance, we assume that the membrane loading is such that the principal membrane stresses are noncompressive. A sufficient condition for this is that $\sigma_{11} \geq 0$ and $\sigma_{11}\sigma_{22} \geq \sigma_{12}^2$.

The mechanical behavior of the membrane will be described by a viscoelastic model with respect to both the deviatoric and equal biaxial (isotropic) stress states. To allow instantaneous strain in response to a suddenly applied stress, an elastic element is connected in series with the Kelvin–Voigt viscoelastic element, as shown in Fig. 1.[2] The two elastic shear moduli are denoted by μ and μ_0, and the two areal moduli are K and K_0 (all in units of N/m). The instantaneous elastic response is governed by the moduli μ_0 and K_0. The shear and areal viscosities are η and $\hat{\eta}$, respectively (in units N s/m). While the stresses are equal in the elastic and viscoelastic elements ($S_{ij} = S_{ij}^{\mathrm{e}} = S_{ij}^{\mathrm{ve}}$; $\sigma_{kk} = \sigma_{kk}^{\mathrm{e}} = \sigma_{kk}^{\mathrm{ve}}$), the strains are obtained as the sum of the elastic and viscoelastic contributions, i.e.,

$$e_{ij} = e_{ij}^{\mathrm{e}} + e_{ij}^{\mathrm{ve}}\,, \quad \varepsilon_{kk} = \varepsilon_{kk}^{\mathrm{e}} + \varepsilon_{kk}^{\mathrm{ve}}\,. \tag{2}$$

The elastic components of strain are related to stress components by Hooke's law[3]

$$e_{ij}^{\mathrm{e}} = \frac{1}{2\mu_0}\,S_{ij}\,, \quad \varepsilon_{kk}^{\mathrm{e}} = \frac{1}{2K_0}\,\sigma_{kk}\,. \tag{3}$$

[1] In a shell-type membrane mechanics, the small thickness (h) of the membrane is included in the analysis via the bending stiffness of the membrane (proportional to $h^2/12$).

[2] Alternatively, a standard linear solid could be considered, in which the Maxwell viscoelastic element is connected in parallel with an elastic element. An elastic and viscous element in series would be a suitable combination to model a permanent deformation of the membrane. For an informative reference to viscoelasticity of biomaterials, see also [12].

[3] If E_0 and ν_0 are the instantaneous Young's modulus and Poisson's ratio of the membrane, then $\varepsilon_{11}^{\mathrm{e}} = (\sigma_{11} - \nu_0\sigma_{22})/E_0$ and $\varepsilon_{22}^{\mathrm{e}} = (\sigma_{22} - \nu_0\sigma_{11})/E_0$, so that $\mu_0 = E_0/2(1+\nu_0)$ and $K_0 = E_0/(1-\nu_0)$. Clearly, $\nu_0 \leq 1$ in the membrane elasticity, where the limiting value $\nu_0 = 1$ corresponds to the membrane that cannot change its area under any loading conditions.

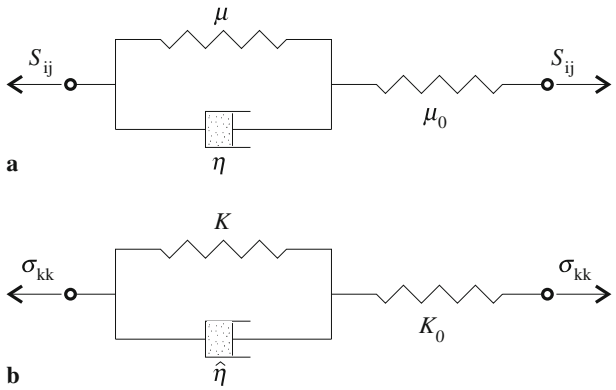

Fig. 1 Mechanical model of a viscoelastic membrane: **a** deviatoric (shear) loading, **b** equal biaxial (isotropic) loading. The instantaneous elastic moduli are μ_0 and K_0, and the two viscosity coefficients are η and $\hat{\eta}$

The viscoelastic components of strain are related to stress by the Kelvin–Voigt type relations

$$S_{ij} = 2\mu e^{\rm ve}_{ij} + 2\eta \dot{e}^{\rm ve}_{ij}\,, \quad \sigma_{kk} = 2K\varepsilon^{\rm ve}_{kk} + 2\hat{\eta}\dot{\varepsilon}^{\rm ve}_{kk}\,, \tag{4}$$

where the superimposed dot designates the time derivative. Upon the combination of (3) and (4), based on (2), the constitutive equations for the in-plane viscoelastic response of the membrane are found to be

$$2\mu e_{ij} + 2\eta \dot{e}_{ij} = \left(1 + \frac{\mu}{\mu_0}\right) S_{ij} + \frac{\eta}{\mu_0}\dot{S}_{ij}\,, \tag{5}$$

$$2K\varepsilon_{kk} + 2\hat{\eta}\dot{\varepsilon}_{kk} = \left(1 + \frac{K}{K_0}\right)\sigma_{kk} + \frac{\hat{\eta}}{K_0}\dot{\sigma}_{kk}\,. \tag{6}$$

By introducing the time-parameters

$$t_* = \frac{\eta}{\mu}\,, \quad \hat{t}_* = \frac{\hat{\eta}}{K}\,, \tag{7}$$

(5) and (6) can be rewritten as

$$e_{ij} + t_*\dot{e}_{ij} = \left(1 + \frac{\mu}{\mu_0}\right)\frac{S_{ij}}{2\mu} + \frac{t_*}{2\mu_0}\dot{S}_{ij}\,, \tag{8}$$

$$\varepsilon_{kk} + \hat{t}_*\dot{\varepsilon}_{kk} = \left(1 + \frac{K}{K_0}\right)\frac{\sigma_{kk}}{2K} + \frac{\hat{t}_*}{2K_0}\dot{\sigma}_{kk}\,. \tag{9}$$

In view of the expressions

$$\begin{aligned} &S_{12} = \sigma_{12}\,, \quad S_{11} = -S_{22} = \frac{1}{2}(\sigma_{11} - \sigma_{22})\,, \quad \sigma_{kk} = \sigma_{11} + \sigma_{22}\,, \\ &e_{12} = \varepsilon_{12}\,, \quad e_{11} = -e_{22} = \frac{1}{2}(\varepsilon_{11} - \varepsilon_{22})\,, \quad \varepsilon_{kk} = \varepsilon_{11} + \varepsilon_{22}\,, \end{aligned} \tag{10}$$

in the subsequent analysis it will be convenient to introduce the following pairs of stress and strain variables:

$$\begin{aligned} &\sigma = \frac{1}{2}(\sigma_{11} + \sigma_{22})\,, \quad S = \frac{1}{2}(\sigma_{11} - \sigma_{22})\,, \\ &\epsilon = \frac{1}{2}(\varepsilon_{11} + \varepsilon_{22})\,, \quad e = \frac{1}{2}(\varepsilon_{11} - \varepsilon_{22})\,. \end{aligned} \tag{11}$$

With these, the constitutive equations (8) and (9) can be recast as

$$t_*\dot{\varepsilon}_{12} + \varepsilon_{12} = \frac{m}{2\mu}\sigma_{12} + \frac{t_*}{2\mu_0}\dot{\sigma}_{12}\,, \tag{12}$$

$$t_*\dot{e} + e = \frac{m}{2\mu}S + \frac{t_*}{2\mu_0}\dot{S}\,, \tag{13}$$

$$\hat{t}_*\dot{\epsilon} + \epsilon = \frac{k}{2K}\sigma + \frac{\hat{t}_*}{2K_0}\dot{\sigma}\,. \tag{14}$$

The utilized dimensionless parameters m and k are

$$m = 1 + \frac{\mu}{\mu_0}, \quad k = 1 + \frac{K}{K_0}. \tag{15}$$

Alternatively, (12), and similarly (13) and (14), can be rewritten as

$$t_* \dot{\varepsilon}_{12} + \varepsilon_{12} = \frac{1}{2\bar{\mu}} \left(\sigma_{12} + \frac{\eta}{\mu + \mu_0} \dot{\sigma}_{12} \right), \tag{16}$$

where $\bar{\mu} = \mu/m$ is the relaxed shear modulus ($\bar{\mu}^{-1} = \mu^{-1} + \mu_0^{-1}$), corresponding to two elastic springs connected in a series.[4]

For a prescribed history of applied stress, and properly specified initial conditions, the differential equations (12)–(14) can be integrated to give the corresponding time variations of strain. The resulting expressions are

$$\varepsilon_{12} = \exp\left(\frac{t_0 - t}{t_*}\right) \left\{ \frac{1}{2\mu} \int_{t_0}^{t} \exp\left(\frac{\tau - t_0}{t_*}\right) \left[\frac{m}{t_*} \sigma_{12}(\tau) + (m-1)\dot{\sigma}_{12}(\tau) \right] \mathrm{d}\tau + \varepsilon_{12}(t_0) \right\},$$

$$e = \exp\left(\frac{t_0 - t}{t_*}\right) \left\{ \frac{1}{2\mu} \int_{t_0}^{t} \exp\left(\frac{\tau - t_0}{t_*}\right) \left[\frac{m}{t_*} S(\tau) + (m-1)\dot{S}(\tau) \right] \mathrm{d}\tau + e(t_0) \right\},$$

$$\epsilon = \exp\left(\frac{t_0 - t}{\hat{t}_*}\right) \left\{ \frac{1}{2K} \int_{t_0}^{t} \exp\left(\frac{\tau - t_0}{\hat{t}_*}\right) \left[\frac{k}{\hat{t}_*} \sigma(\tau) + (k-1)\dot{\sigma}(\tau) \right] \mathrm{d}\tau + \epsilon(t_0) \right\}.$$

The individual longitudinal strains are then determined from $\varepsilon_{11} = \epsilon + e$ and $\varepsilon_{22} = \epsilon - e$, which completes the description of the viscoelastic membrane response in the range of small strains.

3 Loading histories

The closed form solutions for the time variation of strain corresponding to the prescribed loading histories shown in Fig. 2 are given in this Section. The first loading history (Fig. 2a) is a gradual loading to a specified stress level (at constant stress rate), followed by the two intervals of constant stress, released to zero by two consecutive stress drops. The second loading history (Fig. 2b) differs from the previous loading history by the absence of the initial gradual loading stage. The obtained results are used in the parametric study of the infinitesimal creep response of the red blood cell in Sect. 4. Other loading histories, such as those used in the study of the viscoelastic response of polymers [13] may also be of interest, but are not pursued here.

3.1 Gradual loading: stepwise unloading history

The loading history depicted in Fig. 2a is analytically specified by

$$\sigma_{ij} = \begin{cases} \sigma_{ij}^{\circ} t/t_1, & 0 \le t \le t_1, \\ \sigma_{ij}^{\circ}, & t_1 \le t \le t_2^-, \\ \sigma_{ij}^{\bullet}, & t_2^+ \le t \le t_3^-, \\ 0, & t \ge t_3^+. \end{cases} \tag{17}$$

[4] If the standard linear solid was used, in which an elastic spring with shear modulus μ was connected to a Maxwell element (μ_0, η), the equation replacing (16) would read

$$t_* \dot{\varepsilon}_{12} + \varepsilon_{12} = \frac{1}{2\mu} \left(\sigma_{12} + \frac{\eta}{\mu_0} \dot{\sigma}_{12} \right),$$

where $t_* = m\eta/\mu$ and $m = 1 + \mu/\mu_0$. The instantaneous shear modulus in this case is equal to $\mu + \mu_0$, and the relaxed shear modulus is $\bar{\mu} = \mu$.

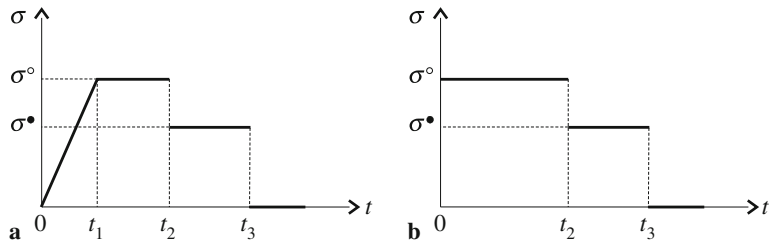

Fig. 2 Two prescribed loading histories

The strain response during the initial steady-state loading range ($0 \le t \le t_1$) is obtained from the general results presented in Sect. 2 as

$$\begin{aligned}
\varepsilon_{12}(t) &= \frac{\sigma^\circ_{12}}{2\mu}\,\frac{t_*}{t_1}\left[m\,\frac{t}{t_*} + \exp\left(-\frac{t}{t_*}\right) - 1\right],\\
e(t) &= \frac{S^\circ}{2\mu}\,\frac{t_*}{t_1}\left[m\,\frac{t}{t_*} + \exp\left(-\frac{t}{t_*}\right) - 1\right],\\
\epsilon(t) &= \frac{\sigma^\circ}{2K}\,\frac{\hat{t}_*}{t_1}\left[k\,\frac{t}{\hat{t}_*} + \exp\left(-\frac{t}{\hat{t}_*}\right) - 1\right].
\end{aligned} \tag{18}$$

In the subsequent time interval, $t_1 \le t \le t_2^-$, the stress is held constant, and the corresponding strains are found to be

$$\begin{aligned}
\varepsilon_{12}(t) &= m\,\frac{\sigma^\circ_{12}}{2\mu}\left[1 - \exp\left(\frac{t_1 - t}{t_*}\right)\right] + \varepsilon_{12}(t_1)\exp\left(\frac{t_1 - t}{t_*}\right),\\
e(t) &= m\,\frac{S^\circ}{2\mu}\left[1 - \exp\left(\frac{t_1 - t}{t_*}\right)\right] + e(t_1)\exp\left(\frac{t_1 - t}{t_*}\right),\\
\epsilon(t) &= k\,\frac{\sigma^\circ}{2K}\left[1 - \exp\left(\frac{t_1 - t}{\hat{t}_*}\right)\right] + \epsilon(t_1)\exp\left(\frac{t_1 - t}{\hat{t}_*}\right).
\end{aligned} \tag{19}$$

At time $t = t_2$ there is a sudden partial unloading from the stress level σ°_{ij} to $\sigma^\bullet_{ij}$. The corresponding sudden decrease in strain is due to the elastic elements with moduli μ_0 and K_0, such that

$$\begin{aligned}
\varepsilon_{12}(t_2^+) &= \varepsilon_{12}(t_2^-) + \frac{1}{2\mu_0}(\sigma^\bullet_{12} - \sigma^\circ_{12}),\\
e(t_2^+) &= e(t_2^-) + \frac{1}{2\mu_0}(S^\bullet - S^\circ),\\
\epsilon(t_2^+) &= \epsilon(t_2^-) + \frac{1}{2K_0}(\sigma^\bullet - \sigma^\circ).
\end{aligned} \tag{20}$$

In the time interval $t_2^+ \le t \le t_3^-$, the stress is held constant at the level $\sigma^\bullet_{ij}$, while the corresponding strains are

$$\begin{aligned}
\varepsilon_{12}(t) &= m\,\frac{\sigma^\bullet_{12}}{2\mu}\left[1 - \exp\left(\frac{t_2 - t}{t_*}\right)\right] + \varepsilon_{12}(t_2^+)\exp\left(\frac{t_2 - t}{t_*}\right),\\
e(t) &= m\,\frac{S^\bullet}{2\mu}\left[1 - \exp\left(\frac{t_2 - t}{t_*}\right)\right] + e(t_2^+)\exp\left(\frac{t_2 - t}{t_*}\right),\\
\epsilon(t) &= k\,\frac{\sigma^\bullet}{2K}\left[1 - \exp\left(\frac{t_2 - t}{\hat{t}_*}\right)\right] + \epsilon(t_2^+)\exp\left(\frac{t_2 - t}{\hat{t}_*}\right).
\end{aligned} \tag{21}$$

Upon the unloading from $\sigma_{ij}^{\bullet}$ to $\sigma_{ij}=0$ at $t=t_3$, the strains are

$$\begin{aligned} \varepsilon_{12}(t_3^+) &= \varepsilon_{12}(t_3^-) - \frac{1}{2\mu_0}\,\sigma_{12}^{\bullet}\,, \\ e(t_3^+) &= e(t_3^-) - \frac{1}{2\mu_0}\,S^{\bullet}\,, \\ \epsilon(t_3^+) &= \epsilon(t_3^-) - \frac{1}{2K_0}\,\sigma^{\bullet}\,. \end{aligned} \tag{22}$$

Finally, in the time interval $t \geq t_3^+$, in which the stresses are held at the zero value, the strains diminish according to

$$\begin{aligned} \varepsilon_{12}(t) &= \varepsilon_{12}(t_3^+)\exp\left(\frac{t_3-t}{t_*}\right), \\ e(t) &= e(t_3^+)\exp\left(\frac{t_3-t}{t_*}\right), \\ \epsilon(t) &= \epsilon(t_3^+)\exp\left(\frac{t_3-t}{\hat{t}_*}\right). \end{aligned} \tag{23}$$

3.2 Sudden loading: stepwise unloading history

The sudden loading—stepwise unloading history, depicted in Fig. 2b, is analytically described by

$$\sigma_{ij} = \begin{cases} \sigma_{ij}^{\circ}, & 0^+ \leq t \leq t_2^-, \\ \sigma_{ij}^{\bullet}, & t_2^+ \leq t \leq t_3^-, \\ 0, & t \geq t_3^+. \end{cases} \tag{24}$$

The instantaneous strain response to a suddenly applied stress σ_{ij}° is

$$\varepsilon_{12}(0^+) = \frac{1}{2\mu_0}\,\sigma_{12}^{\circ}\,, \quad e(0^+) = \frac{1}{2\mu_0}\,S^{\circ}\,, \quad \epsilon(0^+) = \frac{1}{2K_0}\,\sigma^{\circ}\,. \tag{25}$$

In the time interval $0^+ \leq t \leq t_2^-$, the strains accumulate according to

$$\begin{aligned} \varepsilon_{12}(t) &= m\,\frac{\sigma_{12}^{\circ}}{2\mu}\left[1-\exp\left(-\frac{t}{t_*}\right)\right] + \varepsilon_{12}(0^+)\exp\left(-\frac{t}{t_*}\right), \\ e(t) &= m\,\frac{S^{\circ}}{2\mu}\left[1-\exp\left(-\frac{t}{t_*}\right)\right] + e(0^+)\exp\left(-\frac{t}{t_*}\right), \\ \epsilon(t) &= k\,\frac{\sigma^{\circ}}{2K}\left[1-\exp\left(-\frac{t}{\hat{t}_*}\right)\right] + \epsilon(0^+)\exp\left(-\frac{t}{\hat{t}_*}\right), \end{aligned} \tag{26}$$

which can be written condensly as

$$\begin{aligned} \varepsilon_{12}(t) &= \frac{\sigma_{12}^{\circ}}{2\mu}\left[m-\exp\left(-\frac{t}{t_*}\right)\right], \\ e(t) &= \frac{S^{\circ}}{2\mu}\left[m-\exp\left(-\frac{t}{t_*}\right)\right], \\ \epsilon(t) &= \frac{\sigma^{\circ}}{2K}\left[k-\exp\left(-\frac{t}{\hat{t}_*}\right)\right]. \end{aligned} \tag{27}$$

Upon a partial unloading from the stress level σ_{ij}° to $\sigma_{ij}^{\bullet}$, at time $t=t_2$, the strains are

$$\varepsilon_{12}(t_2^+) = \varepsilon_{12}(t_2^-) + \frac{1}{2\mu_0}(\sigma_{12}^{\bullet}-\sigma_{12}^{\circ})\,,$$

$$
\begin{aligned}
e(t_2^+) &= e(t_2^-) + \frac{1}{2\mu_0}(S^\bullet - S^\circ)\,, \\
\epsilon(t_2^+) &= \epsilon(t_2^-) + \frac{1}{2K_0}(\sigma^\bullet - \sigma^\circ)\,,
\end{aligned}
\tag{28}
$$

while in the interval $t_2^+ \le t \le t_3^-$

$$
\begin{aligned}
\varepsilon_{12}(t) &= m\,\frac{\sigma_{12}^\bullet}{2\mu}\left[1 - \exp\left(\frac{t_2 - t}{t_*}\right)\right] + \varepsilon_{12}(t_2^+)\exp\left(\frac{t_2 - t}{t_*}\right), \\
e(t) &= m\,\frac{S^\bullet}{2\mu}\left[1 - \exp\left(\frac{t_2 - t}{t_*}\right)\right] + e(t_2^+)\exp\left(\frac{t_2 - t}{t_*}\right), \\
\epsilon(t) &= k\,\frac{\sigma^\bullet}{2K}\left[1 - \exp\left(\frac{t_2 - t}{\hat{t}_*}\right)\right] + \epsilon(t_2^+)\exp\left(\frac{t_2 - t}{\hat{t}_*}\right).
\end{aligned}
\tag{29}
$$

Upon the complete unloading from $\sigma_{ij}^\bullet$ to $\sigma_{ij} = 0$, at time $t = t_3$, the strains reduce to

$$
\begin{aligned}
\varepsilon_{12}(t_3^+) &= \varepsilon_{12}(t_3^-) - \frac{1}{2\mu_0}\sigma_{12}^\bullet\,, \\
e(t_3^+) &= e(t_3^-) - \frac{1}{2\mu_0}S^\bullet\,, \\
\epsilon(t_3^+) &= \epsilon(t_3^-) - \frac{1}{2K_0}\sigma^\bullet\,.
\end{aligned}
\tag{30}
$$

Thereafter, for $t \ge t_3^+$, they gradually retrieve according to

$$
\begin{aligned}
\varepsilon_{12}(t) &= \varepsilon_{12}(t_3^+)\exp\left(\frac{t_3 - t}{t_*}\right), \\
e(t) &= e(t_3^+)\exp\left(\frac{t_3 - t}{t_*}\right), \\
\epsilon(t) &= \epsilon(t_3^+)\exp\left(\frac{t_3 - t}{\hat{t}_*}\right).
\end{aligned}
\tag{31}
$$

4 Parametric study of the creep response

There have been numerous experiments to measure the elastic and viscous properties of the red blood cell membrane, although different experiments have yielded widely varying results. From micropipette experiments it is estimated that the shear modulus is in the range 5–20 μN/m, while the areal modulus is on the order 10^3–10^4 higher than that [14–17]. In our calculations we adopted the values $\mu = 2\times10^{-5}$ N/m and K =1,000 μ. The relaxation response of the cell from the optical or laser tweezers stretching experiments can also be used to determine the viscoelastic properties of the cell membrane. The characteristic time for relaxation was estimated in this way [18] to be about 0.19 s, somewhat higher than the value of 0.1–0.13 s estimated from micropipette aspiration experiments [2,15]. Based on this data, we adopted in our calculations the shear and areal coefficients of cell viscosity to be $\eta = 2\times10^{-6}$ N s/m and $\hat{\eta} = 100\,\eta$. The areal coefficient of viscosity is chosen so that $\hat{t}_* = 0.1\,t_* = 0.01$ s, which corresponds to a physically reasonable ratio of the two relaxation times.

Consider a uniform loading of the membrane with a positive definite stress state, such that $\sigma_{11}\sigma_{22} \ge \sigma_{12}^2$ and

$$
\sigma_{12} = \begin{cases} \sigma_{12}^\circ, & 0^+ \le t < 5\tau, \\ 0, & t > 5\tau\,, \end{cases}
\tag{32}
$$

where $\tau = \eta/\bar{\mu}$ and $\bar{\mu} = \mu/m$. Using the specified data, as previously indicated, Fig. 3 shows the time variation of the shear strain $\varepsilon_{12}(t)$ for three different values of the parameter m, corresponding to the shear stress (32).[5] The plots illustrate the effect of $m \ge 1$ on the instantaneous elastic response and the subsequent rate of creep.

[5] The shear stress/shear strain response is independent of the superimposed normal stresses and corresponding dilatations.

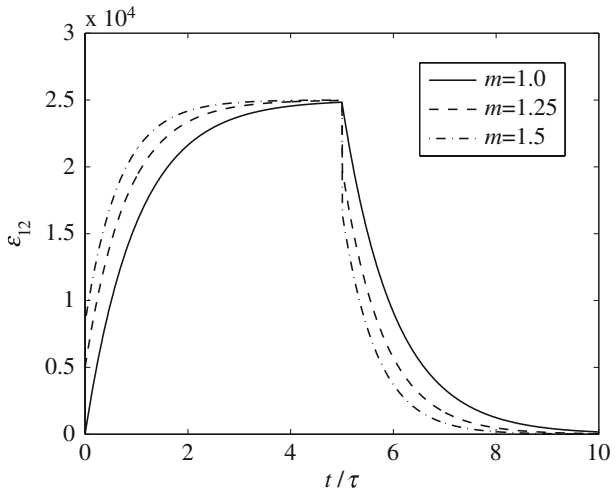

Fig. 3 Time variation of the shear strain $\varepsilon_{12}(t)$ for three different values of the parameter m, corresponding to shear stress history (32)

The value $m = 1$ implies the absence of instantaneous elasticity. The plots are generated by requiring that the saturation strain after long held intervals of constant stress is the same in each case. Physically, this is the most appealing requirement in the study of the creep rates immediately after instantaneous elastic loading or unloading, and was accomplished by rewriting the first expression in (27) as

$$\varepsilon_{12}(t) = \frac{\sigma_{12}^{\circ}}{2\bar{\mu}}\left[1 - \frac{1}{m}\,\exp\left(-m\,\frac{t}{\tau}\right)\right], \tag{33}$$

with $\bar{\mu}$ taken to be constant in each considered case. Accordingly, $\tau = \eta/\bar{\mu}$ is also constant, while $t_* = \tau/m$ is m-dependent. Similar plots can be generated for other loading histories, which include any combination of the inplane stress components.

Consider next a uniaxial tension test in which the stress σ_{11}^0 is suddenly applied at time $t = 0$, while $\sigma_{12} = \sigma_{22} = 0$. Under this loading, $\sigma^0 = S^0 = \sigma_{11}^0/2$, and from (27) there follows

$$e = \frac{\sigma_{11}^0}{4\mu}\left[m - \exp\left(-\frac{t}{t_*}\right)\right], \quad \epsilon = \frac{\sigma_{11}^0}{4K}\left[k - \exp\left(-\frac{t}{\hat{t}_*}\right)\right]. \tag{34}$$

Since $\varepsilon_{11} = \epsilon + e$ and $\varepsilon_{22} = \epsilon - e$, the coefficient of viscoelastic lateral contraction, defined by $c(t) = -\varepsilon_{22}/\varepsilon_{11}$, is

$$c(t) = -\,\frac{\dfrac{1-\nu}{1+\nu}\left[k - \exp\left(-\dfrac{t}{\hat{t}_*}\right)\right] - \left[m - \exp\left(-\dfrac{t}{t_*}\right)\right]}{\dfrac{1-\nu}{1+\nu}\left[k - \exp\left(-\dfrac{t}{\hat{t}_*}\right)\right] + \left[m - \exp\left(-\dfrac{t}{t_*}\right)\right]}, \tag{35}$$

where

$$\frac{1-\nu}{1+\nu} = \frac{\mu}{K}\,.$$

Figure 4a, b show the variation of $c(t)$ corresponding to selected values of the parameters m and k; in Fig. 4a the parameter k is varied at fixed m, while in Fig. 4b the parameter m is varied at fixed k.

If $k = m = 1$, then $\varepsilon_{11}(0^+) = \varepsilon_{22}(0^+) = 0$ (no instantaneous elasticity), and $c(0^+)$ is undetermined. Otherwise,

$$c(0^+) = -\,\frac{(1-\nu)(k-1) - (1+\nu)(m-1)}{(1-\nu)(k-1) + (1+\nu)(m-1)}\,. \tag{36}$$

In particular, for $m = 1$ and $k \neq 1$, $c(0^+) = -1$, while for $k = 1$ and $m \neq 1$, $c(0^+) = 1$. If $k = m \neq 1$, then $c(0^+) = \nu$. The physically unrealistic value $c(0^+) = -1$ for $m = 1$ and $k \neq 1$ is eliminated by including in

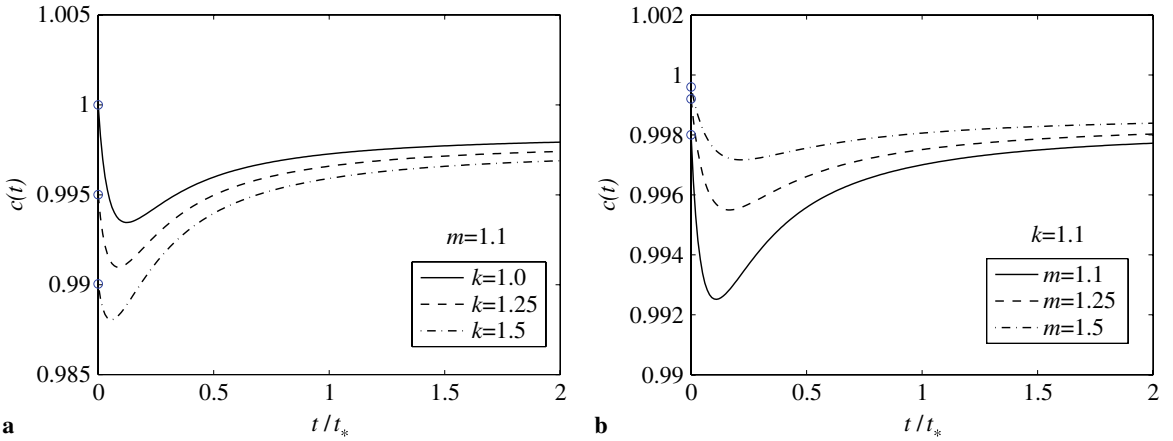

Fig. 4 The variation of the coefficient of viscoelastic lateral contraction $c(t)$. **a** The bulk parameter k is varied at fixed m, **b** the shear parameter m is varied at fixed k

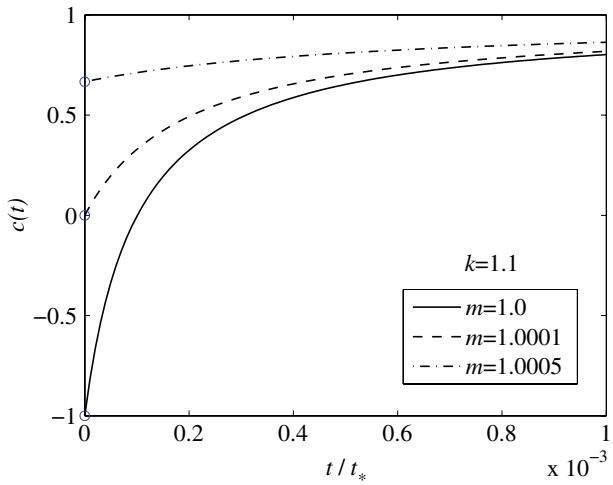

Fig. 5 The variation of the coefficient of viscoelastic lateral contraction $c(t)$, illustrating the effect, via the parameter m, of the instantaneous shear elasticity on the value $c(0^+)$

the model the instantaneous shear elasticity, even with an exceedingly small value of the shear modulus μ_0. This is illustrated in Fig. 5.

If $K \to \infty$ ($\nu \to 1$), then $c(t) \to 1$. If $m = 1$ and $\hat{\eta} \to \infty$ ($\hat{t}_* \to \infty$), then

$$c(t) = -\frac{\dfrac{1-\nu}{1+\nu} - \left[1 - \exp\left(-\dfrac{t}{t_*}\right)\right]}{\dfrac{1-\nu}{1+\nu} + \left[1 - \exp\left(-\dfrac{t}{t_*}\right)\right]}. \tag{37}$$

The two limiting values of the coefficient of viscoelastic lateral contraction are in this case

$$c(0^+) = -1\,, \quad \lim_{t\to\infty} c(t) = \nu\,,$$

which was previously discussed in the literature for materials that exhibit elastic behavior under hydrostatic states of stress and the Kelvin–Voigt viscoelastic behavior under deviatoric states of stress [19].

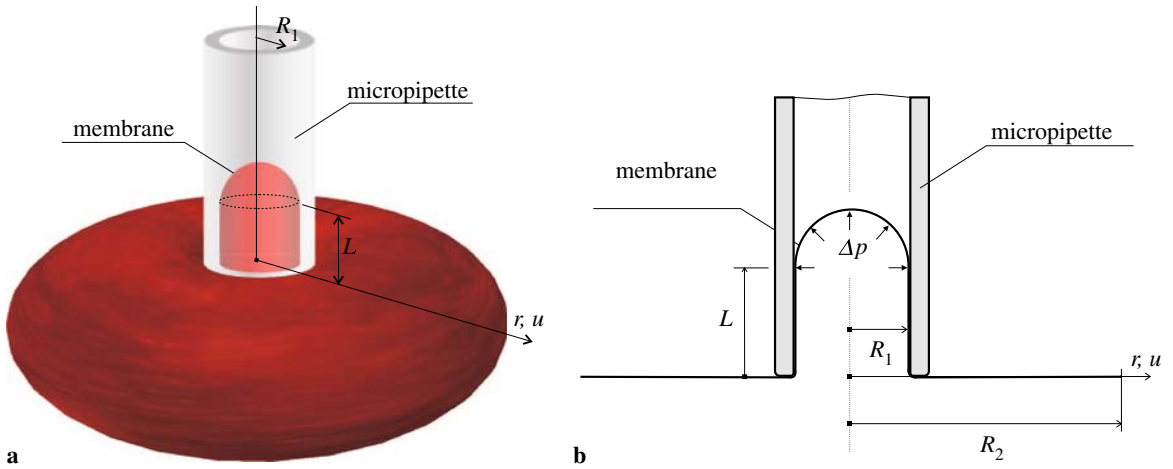

Fig. 6 **a** An approximately axisymmetric biconcave red blood cell under micropipette aspiration in which the cell is being drawn into a glass tube, **b** the suction of an infinite plane membrane into a cylindrical pipette as the model for the experiment

5 Radial stretching of a hollow circular membrane

The characterization of deformation of the red blood cell has been achieved through a variety of experimental techniques. Most common among these methods is the micropipette aspiration technique [2,8], in which the stepwise increase of a suction pressure causes the cell to be drawn into a glass tube, whose inner diameter, in conjunction with the aspiration pressure, can be appropriately chosen so as to control the extent of deformation (Fig. 6).[6] The suction of an infinite plane membrane into a cylindrical pipette is frequently taken as the model for the experiment [15]. If Δp is the pressure difference between the cell and the pipette, the longitudinal stress in the cylindrical portion of the membrane drawn into the pipette is $p = R_1\Delta p/2$. Assuming that the membrane slides smoothly (freely) at the tip of the pipette, the tension over the inner boundary $r = R_1$ of the horizontal flat portion of the membrane is then also equal to p. With this as a motivation, we consider in the subsequent analysis a hollow circular membrane under uniform internal tension of amount p (Fig. 7). The inner and outer radii of the flat membrane are R_1 and R_2, respectively. The outer boundary $r = R_2$ is assumed to be stress-free, although the analysis can be easily extended to include an appropriate membrane tension over the outer boundary to accommodate for the internal pressure in the undeformed biconcave cell. The stress field in the flat membrane throughout the course of infinitesimal viscoelastic deformation is

$$\sigma_r = \frac{R_1^2 p}{R_1^2 - R_2^2}\left(1 - \frac{R_2^2}{r^2}\right), \quad \sigma_\theta = \frac{R_1^2 p}{R_1^2 - R_2^2}\left(1 + \frac{R_2^2}{r^2}\right), \tag{38}$$

independently of the material properties. Introducing

$$\begin{aligned} \sigma &= \frac{1}{2}(\sigma_r + \sigma_\theta)\,, \quad S = \frac{1}{2}(\sigma_r - \sigma_\theta)\,, \\ \epsilon &= \frac{1}{2}(\varepsilon_r + \varepsilon_\theta)\,, \quad e = \frac{1}{2}(\varepsilon_r - \varepsilon_\theta)\,, \end{aligned} \tag{39}$$

where $\varepsilon_r = \mathrm{d}u/\mathrm{d}r$ and $\varepsilon_\theta = u/r$ are the radial and circumferential components of the infinitesimal strain, while $u = u(r, t)$ is the radial displacement, we obtain from (38),

$$\sigma = \frac{R_1^2 p}{R_1^2 - R_2^2}\,, \quad S = -\frac{R_1^2 p}{R_1^2 - R_2^2}\,\frac{R_2^2}{r^2}\,. \tag{40}$$

[6] The human red blood cell has a biconcave shape, with an average diameter of about 8 μm. The cell undergoes large elastic deformations as it passes through narrow capillaries whose inner diameter can be as small as 3 μm. In the process of delivering oxygen from the lungs to body tissues, the red blood cell circulates through the human body nearly half a million times during its life span of about 120 days.

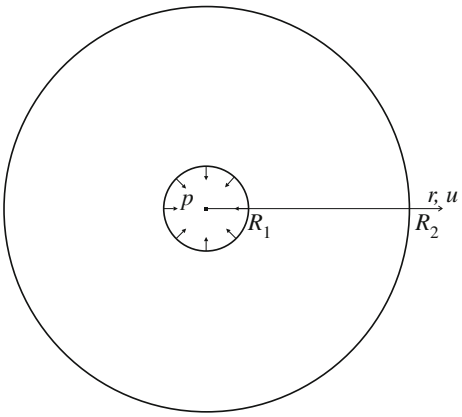

Fig. 7 A hollow circular membrane under uniform tension p applied over the inner boundary $r = R_1$ of the membrane. The outer boundary $r = R_2$ is stress-free

Thus, from (13) and (14), the differential equations for e and ϵ are

$$t_*\dot{e} + e = -\frac{R_1^2}{R_1^2 - R_2^2}\frac{R_2^2}{r^2}\left[\frac{m}{2\mu}p + \frac{t_*}{2\mu_0}\dot{p}\right], \tag{41}$$

$$\hat{t}_*\dot{\epsilon} + \epsilon = \frac{R_1^2}{R_1^2 - R_2^2}\left[\frac{k}{2K}p + \frac{\hat{t}_*}{2K_0}\dot{p}\right]. \tag{42}$$

Suppose that $p = p(t)$ corresponds to a suddenly applied pressure p_0 at time $t = 0$. The solution of Eqs. (41) and (42) is then

$$e(t) = -\frac{p_0}{2\mu}\frac{R_1^2}{R_1^2 - R_2^2}\frac{R_2^2}{r^2}\left[m - \exp\left(-\frac{t}{t_*}\right)\right], \tag{43}$$

$$\epsilon(t) = \frac{p_0}{2K}\frac{R_1^2}{R_1^2 - R_2^2}\left[k - \exp\left(-\frac{t}{\hat{t}_*}\right)\right], \tag{44}$$

analogously to (27). Since $\varepsilon_\theta = \epsilon - e = u/r$, the displacement can be determined from $u = r(\epsilon - e)$, which gives

$$u(r,t) = \frac{p_0}{2\mu}\frac{R_1^2}{R_1^2 - R_2^2}\left\{\frac{\mu}{K}\left[k - \exp\left(-\frac{t}{\hat{t}_*}\right)\right]r + \frac{R_2^2}{r}\left[m - \exp\left(-\frac{t}{t_*}\right)\right]\right\}. \tag{45}$$

The instantaneous elastic displacement field corresponding to sudden application of p_0 is

$$u(r,0^+) = \frac{p_0}{2\mu_0}\frac{R_1^2}{R_1^2 - R_2^2}\left(\frac{1-\nu_0}{1+\nu_0}r + \frac{R_2^2}{r}\right), \tag{46}$$

where ν_0 is the instantaneous Poisson ratio. The variation of $u(r,0^+)/u_0^*$ with r/R_1 and ν_0, in the case $R_2 = 3R_1$, is shown in Fig. 8. The normalizing factor is $u_0^* = p_0 R_1/2\mu_0$. The relevant portion of the shown surface is near $\nu_0 = 1$, because of the exceedingly small areal changes of the cell membrane.

If the areal moduli are infinitely large, (45) simplifies to

$$u(r,t) = \frac{p_0}{2\mu}\frac{R_1^2}{R_1^2 - R_2^2}\frac{R_2^2}{r}\left[m - \exp\left(-\frac{t}{t_*}\right)\right], \tag{47}$$

and in this case

$$u(r,0^+) = \frac{p_0}{2\mu_0}\frac{R_1^2}{R_1^2 - R_2^2}\frac{R_2^2}{r}, \tag{48}$$

$$u(r,\infty) = \frac{p_0}{2\bar{\mu}}\frac{R_1^2}{R_1^2 - R_2^2}\frac{R_2^2}{r}, \quad \bar{\mu} = \frac{\mu}{m} = \frac{\mu_0\mu}{\mu_0 + \mu}. \tag{49}$$

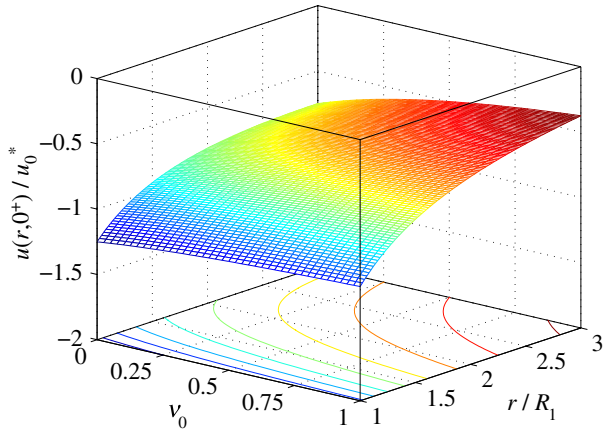

Fig. 8 The variation of $u(r, 0^+)/u_0^*$ with r/R_1 and ν_0, in the case $R_2 = 3R_1$ and according to (46)

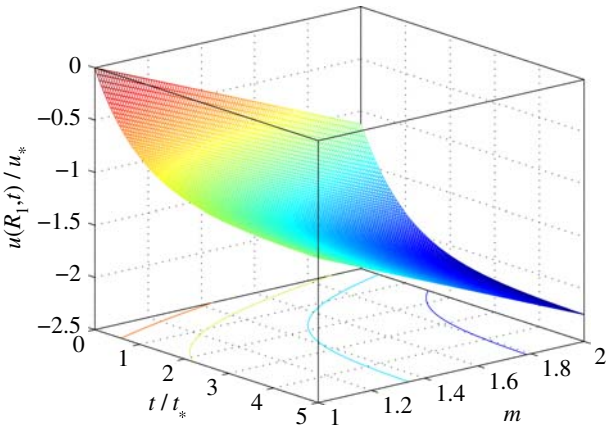

Fig. 9 The normalized displacement $u(R_1, t)/u_*$, versus t/t_* and m, according to (47) and for $R_2 = 3R_1$

The three-dimensional plot of the normalized displacement $u(R_1, t)$, versus time t and the parameter m, for $R_2 = 3R_1$ and according to (47), is shown in Fig. 9. The utilized normalizing factor is $u_* = p_0 R_1/2\mu$. At any instant of time, the normalized displacement u/u_* is a linear function of m, and for a fixed m the magnitude of $u(R_1, t)$ exponentially increases with time, asymptotically approaching the limiting value $mR_2^2/(R_1^2 - R_2^2)$.

If $R_2 \to \infty$, the stresses in the membrane are purely deviatoric, i.e., $\sigma_r = -\sigma_\theta = pR_1^2/r^2$, so that $\sigma = 0$ and $\epsilon = 0$. It readily follows that

$$e(t) = \frac{p_0}{2\mu}\frac{R_1^2}{r^2}\left[m - \exp\left(-\frac{t}{t_*}\right)\right]. \tag{50}$$

Thus, regardless of the areal modulus, the displacement field is

$$u(r,t) = -\frac{p_0}{2\mu}\frac{R_1^2}{r}\left[m - \exp\left(-\frac{t}{t_*}\right)\right], \tag{51}$$

with the limiting values

$$u(r,0^+) = -\frac{p_0}{2\mu_0}\frac{R_1^2}{r}, \quad u(r,\infty) = -\frac{p_0}{2\bar{\mu}}\frac{R_1^2}{r}. \tag{52}$$

The three-dimensional plots of $u = u(r, t)$, corresponding to (51), are shown in Figs. 10 and 11 for the two representative values of the shear parameter $m = 1$ (upper surface) and $m = 1.25$ (lower surface). In the plot in Fig. 11, we held $\bar{\mu}$ and $\tau = \eta/\bar{\mu}$ constant, so that $t_* = \tau/m$ is m-dependent, while in Fig. 10 the shear modulus μ is held constant, so that $\bar{\mu}$ is m-dependent. Accordingly, the time is scaled in this case with fixed t_*,

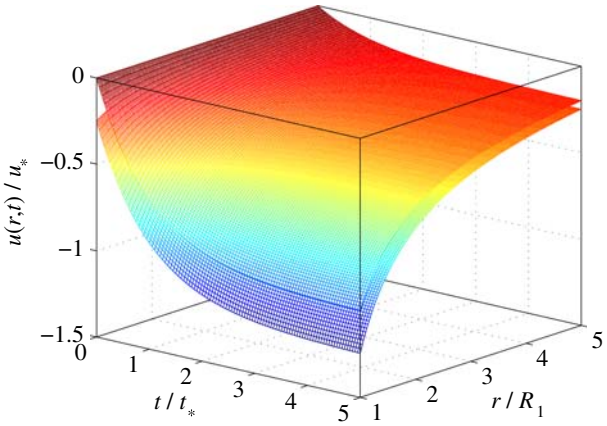

Fig. 10 The three-dimensional plots of $u = u(r, t)$, corresponding to (51) and two representative values of the shear parameter $m = 1$ (*upper surface*) and $m = 1.25$ (*lower surface*). The shear modulus μ is held constant

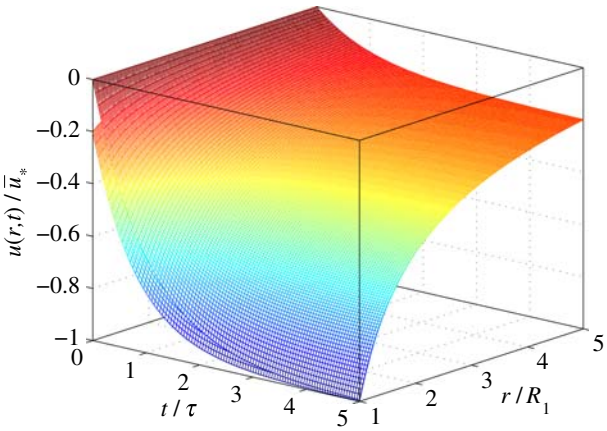

Fig. 11 The three-dimensional plots of $u = u(r, t)$, corresponding to (51) and two representative values of the shear parameter $m = 1$ (*upper surface*) and $m = 1.25$ (*lower surface*). The saturation shear modulus $\bar{\mu}$ is held constant

and the limiting values $u(r, \infty)$ for different m are proportional to m, because $\bar{\mu} = \mu/m$ in (52). A simple relationship holds, $u/u_* = m(u/\bar{u}_*)$. Constraining the saturation shear modulus to be constant in Fig. 11 is analogous to the analysis of the loading portion of Fig. 3 in Sect. 4. This constraint is a preferred choice in the parametric analysis in which the steady state response is prescribed, and the objective is to calibrate the initial elastic response and the subsequent rate of viscoelastic creep by an appropriate selection of m.

The obtained results are of interest for the mechanical analysis of early stages of the micropipette aspiration of red blood cells, and the specification of viscoelastic properties of the cell membrane that remain pertinent in the subsequent nonlinear range of deformation. A detailed analysis of large deformations is essential for the complete mechanical analysis, but can only be performed numerically [21,22]. Large axially symmetric stretching of a nonlinear viscoelastic membrane due to radial stress applied at the outer boundary, by using an integral type constitutive theory, was already considered in [23]. In the context of nonlinear elasticity, a related study of radial deformation of a plane sheet containing a circular hole is presented in [24], where the reference to original work can also be found. For completeness of the present paper, we present in the Appendix a rate-type constitutive theory for large viscoelastic deformations of thin membranes based on the logarithmic finite strain and the loadings along fixed principal directions, as in the considerations of this Section.

6 Concluding remarks

The mechanical behavior of an infinitesimally thin membrane was described by a viscoelastic model with respect to both the deviatoric and isotropic biaxial states of stress. The model also included an instantaneous

elastic response corresponding to a suddenly applied stress. A set of generalized stress and strain variables, defined by a weighted sum and difference of the inplane normal stresses and dilatations, was introduced, which facilitated the derivation and integration of the governing differential equations. Gradual and sudden loading and stepwise unloading histories with a sequential stress drop, were all considered. A parametric study was performed to illustrate the effects of the introduced material parameters on the membrane behavior. The viscoelastic response of a hollow circular membrane under uniform tension applied over its inner boundary was derived without referral to a commonly used correspondence principle from the classical viscoelasticity theory. An extension of the constitutive formulation to large strains is presented in the Appendix of the paper, because large deformation characteristics of living cells significantly affect their biochemical functions [3,20]. A significant amount of work, based on nonlinear elasticity and finite element simulations, was already done in this area to address the evolution of a biconcave shape of the cell during blood flow through small capillaries [21,22]. The adoption of a more comprehensive shell-type membrane elasticity, which includes the bending stiffness of the membrane [6,25–27], may be needed to explain important features of the cell behavior, such as the origin of its shape in the natural healthy state of the cell, or the fatigue and decay of the cell membrane. Damage type theories of inelastic response may be particularly helpful [28,29]. The analysis in this paper may be also of interest in the considerations of other thin membranes, such as nucleus membranes [30] and carbon nanotubes [31]. The incorporation of the inplane elastic anisotropy in the latter case is an important extension of the analysis.

Acknowledgments Research support from the NSF Grant No. CMS-0555280 and the Montenegrin Academy of Sciences and Arts is gratefully acknowledged.

Appendix: A generalization to large viscoelastic deformations

We provide in this Appendix a rate-type constitutive analysis for large viscoelastic deformations of thin membranes based on the logarithmic finite strain measure. Having in mind the applications to radial stretching of membranes, the considerations are restricted to loadings along fixed principal directions.[7] The principal components of the logarithmic strain are defined by

$$\varepsilon_i = \ln \lambda_i \,, \quad i = 1, 2 \,, \tag{A.1}$$

where $\lambda_i \geq 1$ are the principal stretches, the ratios of the deformed and undeformed material length elements in the direction of maximum and minimum stretch. For simplicity we shall adopt the assumption that $\lambda_1 \lambda_2 = 1$, which corresponds to an infinite membrane stiffness to areal changes; ε_i are then necessarily deviatoric ($\varepsilon_1 + \varepsilon_2 = 0$). According to the model in Fig. 1a, we can write

$$\varepsilon_i = \varepsilon_i^{\rm e} + \varepsilon_i^{\rm ve} \,. \tag{A.2}$$

The purely elastic response is assumed to be described by a linear relation between the large logarithmic strain and its work conjugate Cauchy stress, such that[8]

$$\varepsilon_i^{\rm e} = \frac{1}{2\mu} S_i \,, \quad S_i = \sigma_i - \frac{1}{2}(\sigma_1 + \sigma_2) \,. \tag{A.3}$$

Furthermore, since

$$S_i = 2\mu \varepsilon_i^{\rm ve} + 2\eta \dot{\varepsilon}_i^{\rm ve} \,, \tag{A.4}$$

we obtain

$$2\mu \varepsilon_i + 2\eta \dot{\varepsilon}_i = \left(1 + \frac{\mu}{\mu_0}\right) S_i + \frac{\eta}{\mu_0} \dot{S}_i \,, \tag{A.5}$$

where $\dot{\varepsilon}_i = \dot{\lambda}_i / \lambda_i$.

[7] A recent comprehensive review of nonlinear membrane viscoelasticity based on an integral-type constitutive theory was presented in [32].

[8] More commonly, a simple generalization to encompass large elastic deformation is based on adopting the constitutive equations $\sigma_{kk} = 2K\Delta({\rm d}A)/{\rm d}A$ and $\tau_{\max} = 2\mu\gamma_{\max}$, where $\Delta({\rm d}A)/{\rm d}A = \lambda_1\lambda_2 - 1$ is the relative area change, $\gamma_{\max} = (\lambda_2^{-2} - \lambda_1^{-2})/4$ is the maximum (Eulerian) shear strain, and $\tau_{\max} = (\sigma_1 - \sigma_2)/2$ is the maximum shear stress [1]. In general, both K and μ are dependent on λ_1 and λ_2, but, as a first approximation, they are often assumed to be constant [22,33].

For a given strain history, (A.5) can be integrated to give

$$\varepsilon_i = \exp\left(\frac{t_0 - t}{t_*}\right)\left\{\frac{1}{2\mu}\int_{t_0}^{t}\exp\left(\frac{\tau - t_0}{t_*}\right)\left[\frac{m}{t_*}S_i(\tau) + (m-1)\dot{S}_i(\tau)\right]\mathrm{d}\tau + \varepsilon_i(t_0)\right\}, \tag{A.6}$$

where $t_* = \eta/\mu$ and $m = 1 + \mu/\mu_0$. The principal stretches are then calculated as $\lambda_i = \exp(\varepsilon_i)$.
On the other hand, if the deformation history is prescribed, (A.5) can be integrated for S_i to give

$$S_i = \exp\left(\frac{t_0 - t}{T_*}\right)\left\{2\mu\int_{t_0}^{t}\exp\left(\frac{\tau - t_0}{T_*}\right)\left[\frac{1}{mT_*}\varepsilon_i(\tau) + \dot{\varepsilon}_i(\tau)\right]\mathrm{d}\tau + S_i(t_0)\right\},$$

with $T_* = \eta/(m\mu_0)$. The total stress is $\sigma_i = S_i - p$, where $p = p(t)$ is an arbitrary pressure, undetermined by the constitutive analysis of the membrane that is rigid to areal change, but determined by the solution of the specific boundary-value problem.

References

1. Evans, E.A., Skalak, R.: Mechanics and Thermodynamics of Biomembranes. CRC Press, Boca Raton (1980)
2. Hochmuth, R.M., Waugh, R.E.: Erythrocyte membrane elasticity and viscosity. Ann. Rev. Physiol. **49**, 209–219 (1987)
3. Fung, Y.C.: Biomechanics: Mechanical Properties of Living Tissues. Springer, New York (1993)
4. Luisi, P.L., Walde, P. (eds.): Giant Vesicles. Wiley, New York (2000)
5. Boal, D.: Mechanics of the Cell. Cambridge University Press, New York (2002)
6. Pozrikidis, C. (ed.): Modeling and Simulation of Capsules and Biological Cells. Chapman & Hall/CRC, London/Boca Raton (2003)
7. Suresh, S.: Mechanical response of human red blood cells in health and disease: Some structure-property-function relationships. J. Mater. Res. **21**, 1871–1877 (2006)
8. Evans, E.A.: New membrane concept applied to the analysis of fluid shear- and micropipette-deformed red blood cells. Biophys. J. **13**, 941–954 (1973)
9. Christensen, R.M.: Theory of Viscoelasticity: An Introduction. Academic Press, New York (1971)
10. Drozdov, A.D.: Viscoelastic Structures: Mechanics of Growth and Aging. Academic Press, San Diego (1998)
11. Wineman, A., Rajagopal, K.R.: Mechanical Response of Polymers. Cambridge University Press, London (2000)
12. Glasser, W.G., Hatakeyama, H. (eds.): Viscoelasticity of Biomaterials. American Chemical Society, Washington DC (1992)
13. Lubarda, V.A., Benson, D.J., Meyers, M.A.: Strain-rate effects in rheological models of inelastic response. Int. J. Plast. **19**, 1097–1118 (2003)
14. Evans, E.A., Hochmuth, R.M.: Membrane viscoelasticity. Biophys. J. **16**, 1–11 (1976)
15. Chien, S., Sung, K.L.P., Skalak, R., Usami, S., Tozeren, A.: Theoretical and experimental studies on viscoelastic properties of erythrocyte membrane. Biophys. J. **24**, 463–487 (1978)
16. Engelhardt, H., Sackmann, E.: On the measurement of shear elastic-moduli and viscosities of erythrocyte plasma-membranes by transient deformation in high-frequency electric-fields. Biophys. J. **54**, 495–508 (1988)
17. Lenormand, G., Hénon, S., Richert, A., Siméon, J., Gallet, F.: Direct measurement of the area expansion and shear moduli of the human red blood cell membrane skeleton. Biophys. J. **81**, 43–56 (2001)
18. Dao, M., Lim, C.T., Suresh, S.: Mechanics of the human red blood cell deformed by optical tweezers. J. Mech. Phys. Solids **51**, 2259–2280 (2003)
19. Shames, I.H., Cozzarelli, F.A.: Elastic and Inelastic Stress Analysis. Prentice Hall, Englewood Cliffs (1992)
20. Skalak, R., Tozeren, A., Zarda, R.P., Chien, S.: Strain energy function of red blood-cell membranes. Biophys. J. **13**, 245–280 (1973)
21. Lim, C.T., Dao, M., Suresh, S., Sow, C.H., Chew, K.T.: Large deformation stretching of living cells using laser traps. Acta Mater. **52**, 1837–1845 (2004) (with Corrigendum: 4065–4066)
22. Mills, J.P., Qie, L., Dao, M., Lim, C.T., Suresh, S.: Nonlinear elastic and viscoelastic deformation of the human red blood cell with optical tweezers. Mech. Chem. Biosyst. **1**, 169–180 (2004)
23. Wineman, A.: Large axially symmetric stretching of a nonlinear viscoelastic membrane. Int. J. Solids Struct. **8**, 775–790 (1972)
24. Green, A.E., Adkins, J.E.: Large Elastic Deformations. Oxford University Press, New York (1970)
25. Helfrich, W.: Elastic properties of lipid bilayers: theory and possible experiments. Z. Naturforsch. **28C**, 693–703 (1973)
26. Helfrich, W.: Bending elasticity of fluid membranes. In: Luisi, P.L., Walde, P. (eds.) Giant Vesicles, chap. 6, Wiley, New York (2000)
27. Steigmann, D.J.: Fluid films with curvature elasticity. Arch. Rat. Mech. Anal. **150**, 127–152 (1999)
28. Krajcinovic, D., Lubarda, V., Sumarac, D.: Fundamental aspects of brittle cooperative phenomena—effective continua models. Mech. Mater. **15**, 99–115 (1993)
29. Lubarda, V.A.: An analysis of large-strain damage elastoplasticity. Int. J. Solids Struct. **31**, 2951–2964 (1994)
30. Vaziri, A., Mofrad, R.K.: Mechanics and deformation of the nucleus in micropipette aspiration experiment. J. Biomech. **40**, 2053–2062 (2007)

31. Qian, D., Wagner, G.J., Liu, W.K., Yu, M.-F., Ruoff, R.S.: Mechanics of carbon nanotubes. Appl. Mech. Rev. **55**, 495–533 (2002)
32. Wineman, A.: Nonlinear viscoelastic membranes. Comput. Math. Appl. **53**, 168–181 (2007)
33. Asaro, R.J., Lubarda, V.A.: Mechanics of Solids and Materials. Cambridge University Press, Cambridge (2006)